HHS Public Access

Author manuscript

Nat Chem Biol. Author manuscript; available in PMC 2015 December 01.

Published in final edited form as:

Nat Chem Biol. 2015 June ; 11(6): 424–431. doi:10.1038/nchembio.1800.

HIV gp41-Mediated Membrane Fusion Occurs at Edges of Cholesterol-Rich Lipid Domains

Sung-Tae Yang[1,3], **Volker Kiessling**[1,3], **James A. Simmons**[2,3], **Judith M. White**[2,3], and **Lukas K. Tamm**[1,3]

[1]Department of Molecular Physiology and Biological Physics, University of Virginia, Charlottesville, Virginia 22908, U.S.A.

[2]Department of Cell Biology, University of Virginia, Charlottesville, Virginia 22908, USA

[3]Center for Membrane Biology, University of Virginia, Charlottesville, Virginia 22908, USA

Abstract

Lipid rafts in plasma membranes have emerged as possible platforms for entry of HIV and other viruses into cells. However, how lipid phase heterogeneity contributes to viral entry is little known due to the fine-grained and still poorly understood complexity of biological membranes. We used model systems mimicking HIV envelopes and T-cell membranes and showed that raft-like (L_o phase) lipid domains are necessary and sufficient for efficient membrane targeting and fusion. Interestingly, membrane binding and fusion was low in homogeneous L_d and L_o phase membranes, indicating that lipid phase heterogeneity is essential. The HIV fusion peptide preferentially targeted to L_o/L_d boundary regions and promoted full fusion at the interface between ordered and disordered lipids. L_d phase vesicles proceeded only to hemifusion. Thus, we propose that the edges, but not the areas of raft-like ordered lipid domains are vital for HIV entry and membrane fusion.

Biological membranes that separate different compartments within cells as well as the cytosol from the extracellular space are composed of a large variety of lipids, proteins, and cholesterol. Depending on their locations in the cell, membranes have diverse lipid compositions whose roles are still not well understood. From the early fluid mosaic model[1] a much more detailed picture has emerged that describes biological membranes as complex heterogeneous asymmetric lipid bilayer assemblies that are highly crowded with proteins[2, 3]. The lipids in bilayer membranes differ not only by chemical identity but also occur in different thermodynamical states. The term “lipid raft” has been coined for some specialized lipid microenvironments that are enriched in sphingolipids and cholesterol[4, 5]. Lipid rafts have been implicated in a variety of dynamic cellular processes influencing membrane

Corresponding author: Lukas K. Tamm, Tel: +1 434-982-3578, Lkt2e@virginia.edu.

Author Contributions: S-T.Y., V.K., J.M.W. and L.K.T. designed research, S-T.Y. performed most experiments, J.A.S. provided pseudotyped viruses, S-T.Y, V.K., J.M.W. and L.K.T. analyzed data, and S-T.Y., V.K., and L.K.T. wrote paper.

The authors have no competing interests as defined by Nature Publishing Group, or other interests that might be perceived to influence the results and/or discussion reported in this paper.

fluidity, serving as organizing centers for membrane-mediated cell signaling, and regulating the activity of membrane proteins[6]. In addition, lipid rafts have been suggested to play key roles in membrane fusion and fission[7, 8] and increasing evidence has accumulated indicating that lipid rafts serve as platforms for viral entry[9, 10].

Viruses must overcome membrane barriers to deliver the viral nucleocapsid into the cytoplasm. A key step in the entry of enveloped viruses is the fusion of viral membrane envelopes with host membranes[11]. Direct viral fusion with the plasma membrane as well as endocytic pathways have been documented for HIV internalization[12, 13]. The mechanism of viral membrane fusion is a well-studied process[14]. The structures and functions of a number of viral fusion proteins have been characterized to varying degrees of detail[15]. In the case of HIV entry, the gp120 subunit of the viral envelope spike glycoprotein gp120/gp41 first binds to CD4 on the target cell surface. This binding leads to conformational changes within gp120 that allow its additional binding to the CXCR4 or CCR5 co-receptor. A subsequent conformational change in the gp41 subunit exposes its N-terminal fusion peptide and causes it to insert into the cell membrane. An extended intermediate of gp41 then folds back on itself into a hairpin structure, i.e. a process that brings the opposing membranes into close apposition in preparation for membrane fusion[16–18].

Besides proteins, lipids play critical and cooperative roles in the process of membrane fusion during HIV entry[19]. Gp41/gp120 and its receptors and co-receptors are thought to be associated with lipid rafts in the viral envelope and target cell membranes, respectively[20]. Virus infection is inhibited after treatment of cell and viral membranes with methyl-β-cyclodextrin (MβCD) which extracts cholesterol and thus disrupts lipid rafts in these membranes[21]. Cholesterol depletion does not affect the virus's ability to bind target cells, but significantly impairs viral entry[10]. This implies that “rafts” likely play an important role in membrane fusion. However, how cholesterol and associated lipid structures contribute to the mechanism of viral membrane fusion remains to be elucidated.

Lipid rafts are difficult to visualize directly in living cell membranes because of their small size (10~200 nm), their highly dynamic and perhaps only transiently existing nature, and their own heterogeneity, which are all making their study difficult and controversial[6]. Some of these limitations can be overcome under controlled conditions in model membrane systems[22, 23]. In a quest to understand the effects that lipid heterogeneity and rafts might have on the mechanism of viral membrane fusion, we used model membranes with complex lipid mixtures that mimic those of the HIV envelope and T-cell membranes, as well as additional typical lipid mixtures with coexisting liquid-ordered (L_o) and liquid-disordered (L_d) phases, and studied their effects on membrane fusion mediated by the HIV fusion peptide (FP). In these studies we used a version of the FP with a solubilizing C-terminus, which allowed us to deliver the hydrophobic peptides to the fusing membranes from aqueous environments[24, 25] as they are in the full-length protein under physiological conditions. To corroborate our findings, we also examined the targeting of HIV pseudoviruses to structured membranes.

We show that the HIV and T-cell mimicking model membranes exhibit cholesterol-dependent raft-like lipid domains and that the HIV-FP induces membrane fusion of phase-

separated lipid bilayers containing domains more efficiently than fusion of single-phase bilayers in either the L_o or L_d state. The HIV-FP and pseudotyped HIV interact preferentially with boundaries between coexisting L_o and L_d lipid phases and membrane fusion occurs preferentially at these domain boundaries. The results suggest that the edges of lipid rafts play a pivotal role in HIV entry by not only serving as the preferred docking sites, but also as the preferred sites for the opening of fusion pores.

Results

HIV-FP-mediated fusion requires ordered lipid domains

HIV and T-cell membranes are composed of various phospholipids and cholesterol, where the cholesterol/phospholipid molar ratio is about 0.8 in HIV and about 0.4 in T-cell membranes[26]. We first examined how fusion measured by lipid mixing between liposomes prepared from lipid mixtures that mimic the HIV envelope (HIV-lipids: 33.1% SM, 16.0% PC, 35.2% PE, 15.5% PS, and 0.2% other phospholipids, modeled here with all brain lipid species) and liposomes prepared from lipid mixtures that mimic the T-cell membrane (T-cell lipids: 10.4% SM, 43.0% PC, 32.9% PE, 7.4% PS, and 6.3% other phospholipids, modeled here with all brain lipid species) is promoted by the HIV fusion peptide in the presence or absence of cholesterol. HIV-FP induced rapid and efficient lipid mixing between HIV and T-cell lipid liposomes when they contained their natural complements of 0.8 and 0.4 mol/mol cholesterol, respectively (Fig. 1a). However, fusion was significantly reduced when cholesterol was omitted in either the HIV or the T-cell lipid liposomes or both. Images of supported HIV and T-cell lipid monolayers stained with Rh-PE are shown in Supplementary Results, Supplementary Fig. 1. In the absence of cholesterol the HIV lipids exhibit large star-shaped domains, which are typical for gel/L_d phase coexistence[23]. Addition of cholesterol generates round domains, which are typical for L_o/L_d phase coexistence. The fraction of L_o phase increases proportionally to the cholesterol concentration. These results indicate that raft-like L_o phase domains promoted optimal lipid mixing in Fig. 1a. The results are also in good agreement with virus cell entry studies requiring the presence of cholesterol and typical raft lipids for efficient fusion between HIV envelope and T-cell membranes[10, 21].

Next, we reproduced these studies with four simpler lipid compositions, which however are frequently used in model studies on the effects of lipid rafts and lipid phase behavior, namely with liposomes composed of bSM/bPS/Ch (2:1:1) (coexisting L_o and L_d phases), bSM/bPS (3:1) (coexisting gel and L_d phases), and bPC/bPS (3:1) and bPC/bPS/Ch (2:1:1) as single-phase bilayers without and with cholesterol, respectively (Fig. 1b and Supplementary Fig. 2). The phase behavior of corresponding lipid mixtures is shown in Figs. 1c–f. Consistent with the results obtained with HIV and T-cell lipid mixtures, HIV-FP induced most rapid and efficient fusion of L_{o+d} phase bilayers.

To determine whether phase separation in the host or target lipid bilayer was responsible for the enhancement of fusion. We pre-incubated unlabeled liposomes composed of bPC/bPS (3:1) with HIV-FP and added them to fluorescent labeled liposomes composed of bSM/bPS/Ch (2:1:1) or bPC/bPS (3:1). HIV-FP induced lipid mixing with and contents release from bSM/bPS/Ch (2:1:1) liposomes, but not from bPC/bPS (3:1) liposomes (Figs.

1g,h). Increasing concentrations of the raft lipids cholesterol or bSM promoted fusion (Figs. 1i,j). Similarly, depletion of cholesterol in bilayers composed of bSM/bPS/Ch (2:1:1) with MβCD decreased fusion (Fig. 1k) and reduced the appearance of lipid rafts in supported bilayers (Fig. 1l). These results further support the notion that cholesterol-rich L_o phase lipid domains are required for efficient HIV-FP-mediated membrane fusion. Interestingly, bilayers composed of bSM/DPPS/Ch (2:1:1) that form a homogeneous L_o (without a coexisting L_d) phase with slow lipid lateral diffusion (Supplementary Fig. 3a) did not promote HIV-FP-mediated fusion (Supplementary Figs. 3c,d), whereas replacing the saturated chain DPPS with unsaturated chain DOPS in an otherwise identical lipid mixture formed L_o phase domains and promoted fusion (Supplementary Figs. 3b–d).

HIV-FP interacts preferentially with domain boundaries

We reasoned that the increased fusion activity with two-phase ordered/disordered bilayers was the result of increased binding of HIV-FP to such membranes. To test this notion, we employed total internal reflection fluorescence (TIRF) microscopy on supported bPC/bPS (3:1) bilayers with pre-bound HIV-FP to capture liposomes with different phase properties (Fig. 2a). Liposomes composed of bSM/DOPS/Ch (2:1:1, L_{o+d} phases) were captured much more efficiently than liposomes composed of bPC/bPS (3:1, pure L_d phase) or bSM/DPPS/Ch (2:1:1, pure L_o phase) (Fig. 2b). Representative TIRF images of each type of liposomes bound to the supported bilayers are shown in Figs. 2c–e. In addition, when we added in competition experiments L_d or L_o liposomes together with equal amounts of L_{o+d} liposomes, the L_{o+d} liposomes bound preferentially to the HIV-FP-doped supported membranes (Figs. 2f–h).

To determine to which regions of a two-phase lipid bilayer HIV-FP membranes would bind, we turned the configuration of our supported membrane TIRF experiment around as shown in Fig. 2i and used double-label fluorescence microscopy to colocalize liposome binding with different membrane phases. DiD-labeled liposomes composed of bPC/bPS (3:1) were pre-incubated with HIV-FP and then bound to a two-phase supported bilayer composed of bSM/bPS/Ch (2:1:1) that was stained with Rh-PE. The phase structure of the supported bilayer and the bound liposomes were visualized using epifluorescence and TIRF microscopy, respectively (Figs. 2j,k). The overlay shows that most liposomes bound to the boundaries between L_d and L_o phase lipid domains (Fig. 2l). Quantification of HIV-FP targeted liposomes to the different regions of the two-phase bilayer shows that ~5 (1.5) times more liposomes bound to domain boundaries than to L_d (L_o) regions (Supplementary Fig. 4).

To assess if the targeting of HIV-FP liposomes is specific to the sequence of HIV-FP, we performed similar experiments with the fusion peptide of influenza hemagglutinin. Influenza virus enters cells by receptor-mediated endocytosis and requires the low pH of the endosome for fusion and fusion peptide insertion into the membrane[27]. Therefore, these experiments were carried out at pH 5. The binding of liposomes to coexisting L_{o+d} supported bilayers mediated by the influenza fusion peptide did not prefer the L_o/L_d phase boundary region over the L_o or L_d regions of the membrane (Supplementary Fig. 5). Clearly, the HIV-FP is more selective for the phase boundary region than the influenza fusion peptide

(Supplementary Fig. 5d). The lower pH was not responsible for this difference because the HIV-FP still bound to phase boundaries at pH 5. Considering that the endosomal membrane contains less cholesterol than the plasma membrane and is not known to harbor lipid rafts, the indifference of the influenza fusion peptide to raft phase boundaries is physiologically sensible.

HIV-FP-LUVs bind to GUV domain boundaries

To generalize our finding of HIV-FP-mediated domain boundary targeting of large unilamellar vesicles (LUVs) with supported membranes, we examined the same behavior with giant unilamellar vesicles (GUVs)[28]. We pre-incubated DiD-labeled LUVs composed of bPC/bPS (3:1) with HIV-FP and allowed them to bind to Rh-PE-labeled GUVs of the following compositions: bSM/DOPC/Ch (2:2:1) for two-phase L_{o+d} bilayers (Figs. 3a–c), bPC only for uniform L_d phase bilayers (Figs. 3d–f), and bSM/Ch (2:1) for uniform L_o phase bilayers (Figs. 3g–i). After 30 min incubation, numerous bright spots were observed in the DiD channel indicating that many LUVs had bound to the GUVs in a HIV-FP-dependent manner (Fig. 3b). No such interactions were observed in the absence of HIV-FP. Overlaying the images of Figs. 3a,b revealed that most LUVs bound to the domain boundaries of the GUVs composed of bSM/DOPC/Ch (2:2:1) (Fig. 3c). HIV-FP targeted LUVs were not observed on the surface of the single-phase GUVs composed of either bPC or bSM/Ch (2:1) (Figs. 3e,h). The image of another GUV again showed that most LUVs were bound at the phase domain boundary on the L_{o+d} GUV surface (Fig. 3j). When the GUVs and LUVs were both labeled with Rh-PE, we could simultaneously monitor fluctuating dynamic domain boundaries on the GUV surface and the relative positions of LUVs bound to these boundaries (Supplementary Video 1). The LUVs (indicated by yellow arrows in Fig. 3k) moved along the L_o/L_d boundaries on the GUV indicating that the HIV-FP-bound LUVs remained confined to the boundary, even if this line was moving on the vesicle.

An NBD-labeled HIV-FP analog also binds preferentially to two-phase LUVs and GUVs (Supplementary Fig. 6). As explained in Supplementary Results to this figure, the peptides remained bound to their original liposomes and did not migrate from one liposome to another. When the HIV-FP was bound to GUVs, long lipid tubules grew out from the L_o/L_d boundary regions (Supplementary Fig. 7). Similar effects were not observed on single phase L_d or L_o GUVs. Although interesting, this tubulation process was not further investigated at this time.

HIV-FP-liposomes fuse at L_o/L_d phase boundaries

Having established that HIV-FP-liposomes preferentially target L_o/L_d phase boundaries, we wanted to know whether these were also the sites of fusion. To this end, we prepared Rh-PE-labeled supported bilayers composed of bSM/bPC/Ch (2:2:1), which mimics the outer leaflet of host cell membranes, and observed by TIRF microscopy individual fusion events[29] of DiD-labeled liposomes composed of HIV lipids (L_{o+d} mixture as in Fig. 1a, Figs. 4a–c), bSM/DOPS/Ch (2:1:1, standard L_{o+d} mixture, Figs. 4d–f), bPC/bPS (3:1,L_d mixture, Figs. 4g–i), or bSM/DPPS/Ch (2:1:1, L_o mixture, Figs. 4j–l). The supported membranes were pre-incubated with HIV-FP before the liposomes were added. Although all four types of liposomes bound to domain boundaries on the supported membranes as expected, only the

two-phase L_{o+d} liposomes (Figs. 4a–f), but not the single-phase L_d or L_o liposomes (Figs. 4g–l) fused efficiently with the supported membrane. In these experiments, fusion was observed by mixing of DiD with the supported membrane[29], which resulted in a rapid spread and equilibration into the L_d regions and a more readily observable slower spread of growing round fluorescent domains in the L_o phase domains (Supplementary Video 2 and Supplementary Fig. 8).

We analyzed ~4,400 individual liposome fusion events by plotting peak fluorescence intensities from individual liposomes as a function of time. We observed three distinct behaviors: a fluorescence intensity that did not change with time (Fig. 4m), a complete decay of the fluorescence intensity (Fig. 4n), and a fluorescence intensity decay to around one half of the original peak intensity (Fig. 4o). We assign these behaviors to docking, full fusion, and hemifusion events, respectively. Selected TIRF images of the time evolution of individual liposomes visualize each behavior (Figs. 4m–o). To further prove that the liposomes with the behavior shown in Fig. 4n indeed were undergoing full fusion, we prepared DiD-labeled liposomes, which were also loaded with the water-soluble fluorescent dye sulforhodamine B to measure content release upon fusion[30]. Two-phase supported bilayers composed of bSM/bPC/Ch (2:2:1) were labeled with NBD-DPPE, which preferentially partitions into the L_o phase[23] and lipid mixing and the release of sulforhodamine B from fusing HIV lipid liposomes were tracked by following the fluorescence intensities in and around individual liposomes. The three-color experiment presented in Fig. 4p shows that the content dye of a L_{o+d} liposome that bound to a domain edge and hemifused at time 0 was released upon full fusion after 32.2 seconds into the space under the supported membrane, providing direct proof for complete membrane fusion. The sulforhodamine B signal decreased approximately exponentially over a period of 3.8 seconds, which can only be explained by a graded release through a fusion pore and is inconsistent with vesicle rupture, which would have resulted in a dissipation of the fluorescence from its origin within milliseconds. A movie of this process is shown in Supplementary Video 3.

The relative frequencies of the different types of events shown in Figs. 4m–o are plotted in the bar graphs shown in Fig. 4q. Although similar numbers of the different types of liposomes (1307 for HIV lipids, 1182 for L_{o+d} phase liposomes, 1062 for L_d phase lipids, and 903 for L_o phase lipids) were analyzed for fusion on supported membranes, HIV-FP did not induce fusion of liposomes in the L_o phase and only 18% of liposomes in the L_d phase exhibited membrane fusion including hemifusion. In contrast, 72±6% of the HIV lipid and 64±7% of the model L_{o+d} liposomes fused that were bound at domain boundaries. Therefore, phase coexistence in both the target and liposome membrane was required for efficient membrane fusion to occur.

Activated HIV Env pseudoviruses target domain boundaries

In order to test whether HIV particles would also target phase boundaries in heterogeneous target membranes, we prepared murine leukemia virus particles pseudo-typed with HIV-1 envelope protein and investigated their binding to phase-separated membranes composed of bSM/DOPC/Ch (2:2:1). Since in native gp120/gp41 the fusion peptide is buried within the

envelope protein and since no receptors were included in the target membrane, little binding of HIV pseudoviruses to these membranes was observed. However, when the envelope glycoprotein was activated to expose the fusion peptide by mild heat and enfuvirtide treatment, strong binding to the boundaries between L_o and L_d phases was observed in supported bilayers (Figs. 5a–c) and GUVs (Figs. 5d–f). Quantification of the data shown in Figs. 5a–c and statistics that include additional repeat experiments are presented in Supplementary Table 1. Enfuvirtide is known to stabilize the activated structure of gp41 that features an exposed fusion peptide by interfering with the formation of the fusion promoting helical hairpin between heptad regions 1 and 2 of gp41[31]. Since there was little binding of HIV pseudoviruses to the membranes in the absence of heat/enfuvirtide activation, the preference of the viruses to bind to the boundary regions is most likely mediated by the fusion peptide of gp41.

Discussion

In this work we developed a molecular understanding of why cholesterol and cholesterol-induced lipid phase heterogeneity in membranes is important for the insertion of the fusion peptide of HIV gp41 and its ability to fuse membranes. Although “lipid rafts” in cell membranes and the high concentration of cholesterol in HIV envelopes have long been implicated as important factors contributing to cell entry, the molecular reasons for this requirement were not well understood. This is not surprising because lipid rafts are still ill defined in terms of lipid composition, size, and longevity, and there is mounting evidence that many kinds of different raft-like structures co-exist in cell membranes. This unsatisfactory situation prompted us to take a reconstitution approach to develop in vitro model membranes with complex, but well controlled and well-defined lipid configurations. This approach allowed us to study the effects of many different lipids in the context of structured lipid bilayers that should mimic those encountered in cell membranes albeit at larger length scales that are amenable to investigation by optical microscopy. Using a combination of supported and liposomal model membranes revealed novel molecular interactions of the HIV fusion peptide with membrane constituents that were organized in complex fabrics resembling those of cell membranes and to define supra-molecular requirements for the promotion of membrane fusion that would be difficult to observe by other means.

The HIV fusion peptide promoted most efficient fusion between liposomes containing lipid mixtures that separate into co-existing ordered and disordered phases, such as those present in the HIV envelope and target T-cell membranes. Lipid phase-separation in the target membrane is more important than in the host (viral) membrane for efficient fusion to proceed. Ordered or disordered single-phase target membranes fuse less easily than two-phase membranes, even if they contain equal amounts of cholesterol. This proves that cholesterol is necessary, but not sufficient, and that its context with other lipids matters to promote efficient fusion.

The reason for fusion promotion in two-phase membranes can be traced to our finding that liposomes decorated with the HIV-FP preferentially target L_o/L_d phase boundaries in supported lipid bilayers and GUVs. Both systems essentially yielded the same results, but

there are some technical differences. The GUV system has the advantage that possible adverse effects of the quartz support that may occur in the supported bilayer experiments are eliminated. Since domain boundaries are mobile in GUVs, we were also able to follow by epifluorescence microscopy bound liposomes as they moved with the domain boundaries. On the other hand, the supported bilayers are planar, permitting the acquisition by TIRF microscopy of much larger datasets and statistics to quantify the liposome-boundary interactions.

We found that HIV-FP decorated liposomes not only bind to L_o/L_d phase boundaries, but also fuse preferentially at these boundaries. Fusion to pure L_o and L_d phase membranes was much less frequent. Our single liposome fusion assay also allowed us to distinguish between full and hemifusion events. Quite interestingly, we found that HIV-FP-promoted fusion resulted in mostly hemifusion events with pure L_d phase target membranes, but full fusion was prevalent at the L_o/L_d phase boundaries.

Although our experiments were carried out at room temperature, they are also highly relevant to situations at 37°C. Nanoscale lipid rafts are observed in living cell membranes at physiological temperature[32] and raft-like domains persist in model membranes up to physiological temperatures[33]. Critical fluctuations are observed a few degrees below 37°C in model membranes and plasma membrane-derived vesicles[34, 35] and these lipid heterogeneities are stabilized to persist to at least 37°C by adhesion and interactions with the cytoskeleton[36, 37]. This behavior makes interfaces between ordered and disordered lipids even more prevalent in these systems than in neatly phase-separated bilayers. Therefore, our finding that HIV gp41 prefers ordered/disordered lipid interfaces for entry by membrane fusion is at least as relevant at 37C as observed here at room temperature.

We recognize that HIV-FP-mediated fusion may not capture the full story of fusion mediated by the entire gp120/gp41 fusion protein. HIV-FP insertion into target membranes only occurs after binding of gp120 to its receptor and co-receptor. There is no question that additional factors such as the distribution of the envelope protein in the viral envelope and the distribution of the receptor and co-receptor in the host cell membranes may play additional significant roles in selecting appropriate sites for fusion in complex target membranes. However, as discussed by many, raft-like lipid assemblies in cell membranes may be very small, perhaps even as small as a few dozen lipid molecules[7, 38]. This would make interfaces between such lipid clusters much more frequent in cell membranes than in model membranes and may make these interfaces much easier to reach from any location in the membrane. However, the guiding physical principles for FP insertion, membrane bending, and ultimately fusion would still be the same as visualized here in the reconstituted lipid systems that exhibit phase separations on larger optically resolvable length scales.

Figure 6 illustrates possible connections of domain boundary targeting in the biological system (Fig. 6a) and the reduced lipid model membrane system with just the HIV fusion peptide as the fusogen (Figs. 6b,c). When HIV binds to its receptors on the cell membrane and gets activated for fusion, gp41 extends from a raft-like viral envelope in a pre-hairpin conformation, in which the fusion peptides are projected towards the target membrane (Fig. 6a, see also ref. 18). Since the CD4 receptor and the chemokine co-receptors are also

thought to be recruited to lipid rafts in the host cell membrane, the binding of HIV would therefore bring ordered lipid domains of the virus and host cell membranes into close proximity. The interaction of the FP with a phase boundary in the host membrane leads to three possible configurations of virus-host membrane contacts: L_d-boundary, L_o-boundary, and boundary-boundary (Fig. 6b). Our results showed that the boundary-boundary contact provided the most efficient configuration for membrane fusion, while fusion in the other configurations proceeded only to hemifusion (L_d-boundary) or was virtually not observed (L_o-boundary).

Why are lipid domain boundaries beneficial for membrane fusion? Membrane fusion costs energy: membranes need to bend, water needs to be removed between the two fusing membranes, and lipids need to assume non-bilayer conformations, which all are energetically disfavored in single phase lipid bilayers. The energy required to drive membrane fusion is thought to be provided by the refolding of the fusion protein and by the insertion of the fusion peptides into the host bilayer. The boundaries between different lipid phases are the favored sites for fusion peptide insertion and also likely present “fault lines” for membrane deformations. Specifically, (1) fusion peptides preferably insert at the edges of raft domains where they likely also self-associate into larger oligomeric structures[39, 40] as they are always delivered in multiples of three because of the trimeric structure of the fusion protein; (2) lipid mismatch at L_o/L_d interfaces that is likely asymmetric due to the one-sided insertion of the fusion peptides induces membrane curvature and thereby reduces the free energy of curved membrane fusion intermediates; (3) the topological discontinuity at the interface between L_o and L_d phases creates line tension[41, 42], which may be relieved and provide energy upon membrane fusion; (4) the boundary-boundary contact across two lipid bilayers is energetically favorable[43, 44] and may lead to favorable domain coalescence between these bilayers, which could promote membrane fusion; and (5) lipid asymmetries between viral and target membranes could favor hemifusion intermediates requiring shifting mismatched domain boundaries between the two leaflets back into register, which would promote full fusion. A progression of membrane fusion at lipid domain boundaries is illustrated in Fig. 6c.

The effect of lipid rafts and especially raft domain boundaries on HIV-FP-mediated membrane fusion described in this work may not be limited to this particular fusion system, but may be much more general. Lipid phase heterogeneity and edge effects of lipid rafts have recently been shown to change our current thinking of how lipidated signaling molecules like Rac1 are translocated to membranes[45]. Membrane discontinuities at the edges of rafts may affect membrane fusion in the entry pathways of not only HIV, but also other enveloped viruses and may play a role in intracellular vesicle fusion in membrane trafficking in healthy cells. Cholesterol-dependent lipid and protein clusters – in lipid raft or non-raft associations – have been implicated in neurotransmitter release at synapses[46], neuronal SNARE protein assemblies[47], the formation of multinucleated myotubes[48] and osteoclasts[49], and in sperm-egg cell fusion[50]. It will be interesting to see to what other fusion systems the conclusions of this work can be extended in the future. The tools that we have developed here should facilitate many exciting future investigations of lipid domain edge effects in viral and non-viral membrane fusion.

ONLINE METHODS

Materials

All lipids including fluorescent probes were from Avanti Polar Lipids (Alabaster, AL). The only exceptions were 1,1'-dioctadecyl-3,3,3',3'-tetramethylindodicarbocyanine perchlorate (DiD), aminonaphthalene-1,3,6-trisulfonic acid (ANTS), and p-xylene-bis-pyridinium bromide (DPX), which were from Molecular Probes (Invitrogen, Carlsbad, CA). Cholesterol, MβCD, and 4-chloro-7-nitrobenzofurazan (NBD-Cl) were purchased from Sigma (St. Louis, MO). 1,2-dimyristoyl-phosphatidylethanolamine-N-(polyethylene glycol-triethoxysilane) (DPS) and the HIV-FP with the sequence AVGIGALFLGFLGAAGSTMGAASGGGKKKKK were custom synthesized by Shearwater Polymers (Huntsville, AL) and by the Yale W.M. Keck Biotechnology Resource Laboratory (New Haven, CT), respectively.

Preparation of liposomes

Large unilamellar vesicles (LUVs) were prepared by the extrusion technique. In brief, the desired amounts of lipids dissolved in chloroform or chloroform/methanol were mixed and the solvent was evaporated under a stream of nitrogen gas in a glass test tube. The lipid film was further dried under vacuum overnight and hydrated with 0.5 ml HEPES buffer (10 mM HEPES, 120 mM NaCl, pH 7.2). The resulting suspension was subjected to ten cycles of freezing and thawing using liquid nitrogen and warm water and thereafter extruded 21 times through two stacked polycarbonate filters of 100 nm pore-size (Avestin, Ottawa, ON). Giant unilamellar vesicles (GUVs) were prepared by the electroformation technique[51]. In brief, 25 l of a 10 mM lipid solution in organic solvent containing the fluorescent lipid probe Rh-PE (0.1 mol%) was deposited on clean glass slides that were coated with indium tin oxide and then placed in vacuum for 90 min to eliminate residual solvent. The fabrication chamber filled with 300 mM sucrose in H_2O was composed by two conducting slides separated by a spacer of 0.5 mm. Electroformation was performed at around 60°C by applying alternating electric current (3 V, 10 Hz) for 120 min. The GUVs were transferred into a 300 mM glucose solution to let them settle by gravity on the microscope slide.

Preparation of supported lipid monolayers and bilayers

Quartz slides (Quartz Scientific, Fairport Harbor, OH) were cleaned by boiling in Contrad detergent for 15 min and then sonicated for 30 min in a hot bath. After rinsing with water and ethanol, remaining organic residues were removed by Piranha solution (3:1 of 95% H_2SO_4 and 30% H_2O_2), followed by extensive rinsing in pure water. Lipid mixtures were spread onto a pure water surface in a Nima 611 Langmuir-Blogdett trough (KSV NIMA, Espoo, Finland). Solvent was allowed to evaporate for 10 min at a surface pressure of 5 mN/m and then the monolayer was compressed at a rate of 10 cm^2/min to reach a surface pressure of 32 mN/m. The quartz slides were further cleaned immediately prior to use for 10 minutes in an argon plasma sterilizer (Harrick Scientific, Ossining, NY) and then dipped into the trough with a speed of 200 mm/min and withdrawn at 5 mm/min while keeping the surface pressure constant at 32 mN/m. This transferred a single lipid monolayer onto the quartz support. Polymer (PEG)-supported lipid bilayers were formed by a combined Langmuir-Blodgett/LUV fusion (LB/VF) technique as previously described[52]. Each LB

monolayer contained 3 mol% of the 77 ethylene glycol unit-containing reactive lipid DPS to link the polymer and lipid covalently to the SiO_2 surface of the quartz slide. The slide was dried in a vacuum desiccator at room temperature overnight and cured in a 70 °C oven for 40 min. After equilibration in a desiccator at room temperature, the slide with the tethered polymer-supported LB monolayer was placed in a custom-built flow-through chamber. A 0.1 mM suspension of LUVs in HEPES buffer was injected into the chamber and incubated for at least 2 hours at room temperature. Excess LUVs in the chamber were washed out by extensive rinsing with HEPES buffer. Typically only the top monolayer contained 0.1 mol% Rh-PE or 0.5 mol% NBD-PE. Otherwise and with the exception of DPS in the bottom monolayer, the lipid compositions of both leaflets were identical.

Binding of NBD-labeled HIV-FP to vesicles

1 mM HIV-FP was reacted with 2 mM NBD-Cl in borate buffer (50 mM borate, 20 mM EDTA, pH 8.0) for 1 hour at room temperature. Uncoupled dye was removed by gel filtration on a PD-10 column. To measure the binding of NBD-labeled peptides to LUVs with different lipid phases, the LUVs were added successively to 0.5 M NBD-HIV-FP in HEPES buffer. The fluorescence emission spectra were recorded with a Jobin-Yvon Fluorolog-3 spectrofluorometer (Jobin-Yvon, Edison, NJ) with excitation at 475 nm and the intensities at 530 nm were measured as a function of the lipid-to-peptide molar ratio. To visualize the binding of HIV-FP to phase-separated GUVs, 1 M NBD-HIV-FP was incubated for 30 min at room temperature with GUVs that were labeled with Rh-PE.

Liposome lipid mixing and content release induced by HIV-FP

The lipid mixing assay was based on a commonly used fluorescence resonance energy transfer (FRET) assay[53]. LUVs were added to a cuvette in a ratio of 1:9 of labeled (1 mol% Rh-PE and NBD-PE each) to unlabelled LUVs to give a total lipid concentration of 50 μM in HEPES buffer at room temperature. Lipid mixing induced by HIV-FP was recorded under constant stirring using the Fluorolog-3 spectrofluorometer with the excitation and emission wavelengths set at 460 nm and 535 nm, respectively. To measure content release, LUVs were prepared in a buffer solution containing the small water-soluble fluorescent dye ANTS together with the quencher DPX (12.5 mM ANTS, 45 mM DPX, 50 mM NaCl, 10 mM HEPES, pH 7.2). Unencapsulated dyes and quenchers were removed by size exclusion chromatography using a PD-10 desalting column (Amersham Biosciences, Piscataway, NJ). Content release induced by the HIV-FP was recorded under constant stirring using the Fluorolog-3 spectrofluorometer with the excitation and emission wavelengths set at 355 nm and 520 nm, respectively. The 0% lipid mixing or content release marks were the fluorescence intensities of the LUV suspension before HIV-FP was added and the 100% levels of complete lipid mixing or content release were defined by the fluorescence intensities produced after the addition of 0.5% (v/v) Triton X-100 to the reactions.

Visualization of HIV-FP-mediated binding of LUVs to GUVs

To visualize the binding of LUVs to GUVs mediated by the HIV-FP, GUVs were labeled with 0.1 mol% Rh-PE and LUVs were labeled with 0.5 mol% DiD. HIV-FP was incubated with LUVs (peptide:lipid molar ratio of 1:50) for 10 min and then injected into the chamber containing the GUVs. The binding of LUVs to GUVs was monitored by epifluorescence

microscopy. Images were recorded on a Zeiss Axiovert 200 fluorescence microscope (Carl Zeiss, Thornwood, NY) with a mercury lamp as a light source, a 63× water immersion objective (Carl Zeiss; NA = 0.95), and an electron multiplying charge-coupled device (EMCCD) cooled to −70 °C (iXon DV887ESC-BV, Andor, Belfast, U.K.) as a detector. Images were acquired using homemade software written in LabVIEW (National Instruments, Austin, TX). Bilayers stained with NBD were illuminated through a 480 nm band-pass filter (D480/30, Chroma, Brattleboro, VT) and via a dichroic mirror (505dclp, Chroma) through the objective. Fluorescence was observed through a 535 nm band-pass filter (D535/40, Chroma). Rhodamine-stained bilayers were illuminated through a 540 nm band-pass filter (D540/25, Chroma) and via a dichroic mirror (565dclp, Chroma) through the objective. Fluorescence was observed through a 605 nm band-pass filter (D605/55, Chroma). LUVs stained with DiD were illuminated through a 620 nm (ET620/60, Chroma) and via a dichroic mirror (660dclp, Chroma), and observed through a 665 nm band-pass filter (HQ665/60, Chroma). All images were obtained at room temperature.

Visualization and quantification of HIV-FP-mediated binding of LUVs to supported lipid bilayers

To measure the binding efficiency of LUVs to supported lipid bilayers mediated by the HIV-FP, the bilayers were incubated with 5 M HIV-FP for 10 min at room temperature and then unbound peptides were washed away with HEPES buffer. 2 M of LUVs labeled with 0.5 mol% DiD were added to the supported membranes. To investigate the targeting of LUVs to different regions of L_d/L_o phase-separated supported membranes, the LUVs and bilayers were labeled with 0.5 mol% DiD and 0.1 mol% Rh-PE, respectively. HIV-FP was incubated with LUVs (peptide:lipid molar ratio of 1:50) for 10 min and then injected into the chamber with the supported membrane. To monitor the binding of LUVs to the supported bilayer by TIRF microscopy, a focused laser beam (CUBE 640-40C, Coherent, Palo Alto, CA) was directed through a trapezoidal prism onto the quartz−buffer interface where the supported bilayer was attached. The prism−quartz interface was lubricated with glycerol to allow easy translation of the sample chamber on the microscope stage. The laser beam was totally internally reflected at an angle of 72° from the surface normal, producing an evanescent wave that decays exponentially in the solution with a characteristic penetration depth of 90 nm. The intensity of the laser beam was modulated by the computer or could be completely blocked by a computer-controlled shutter (Vincent Associates, Rochester, NY). Images were recorded by an EMCCD (iXon DV887ESC-BV, Andor). Data acquisition and image analysis from TIRF microscopy were accomplished through custom-built software written in LabVIEW (National Instruments, Austin, TX)[54]. To analyze and quantify the distribution of membrane-bound liposomes, we distinguished between three regions of the supported membranes: L_o domains, L_d phase areas, and boundary regions with a 0.75 μm width centered on the perimeter of each L_o domain. Custom-built particle tracking software[54] was used to automatically detect the position (x/y coordinates) of each liposome

HIV-FP-mediated fusion of single liposomes to supported lipid bilayers

To monitor fusion of single liposomes with supported lipid bilayers, the supported membranes were incubated with 5 M HIV-FP for 10 min at room temperature and then unbound peptides were washed away with HEPES buffer. 2 M of LUVs labeled with 0.5

mol% DiD were added to the supported membranes. To monitor content mixing, LUVs were prepared in a buffer solution containing water-soluble fluorescent sulforhodamine B (10 mM HEPES, 50 mM sulforhodamine B, pH 7.2, adjusted to 250 mmol/kg osmolality by addition of NaCl). Unencapsulated dye was removed by running the liposomes through a PD-10 desalting column. Docking and fusion of individual liposomes to the supported membrane were monitored by TIRF microscopy using a diode laser (CUBE640, Coherent) and an argon ion laser (Innova 90C-5, Coherent) at the same time[30]. Single fusion events were analyzed as described in previous references[29, 30].

Binding of HIV pseudovirus to phase-separated membranes

Viral particles pseudotyped with a murine leukemia virus (MLV) core and the HIV-1 envelope protein were prepared by co-transfection of 293T cells with 3 g pFB-Luc (reporter plasmid), 2 g pHIT60 (MLV-gag-Pol), 1 g MLV gag-mKO (gift of G. Melikyan), and 3 g HIV-1 JRFL Env plasmids per 10 cm culture dish. Viral supernatants were harvested 48 hours after transfection and centrifuged at 2500 rpm for 10 min at 4C. They were flash-frozen and stored at –70 C for later use. Supported lipid bilayers or GUVs composed of bSM/DOPC/Ch (2:2:1) were labeled with 0.1 mol% DiD. The viruses were incubated for 30 min at 55 C in the presence of 10 g/ml enfuvirtide (Sigma, St. Louis, MO) and brought back to room temperature. After equilibration at room temperature, the viruses were added to supported bilayers or GUVs. The heat/enfuvirtide treatment was omitted in control experiments. mKO-labeled HIV pseudoviruses were illuminated through a 540 nm band-pass filter (D540/25, Chroma) and dichroic mirror (565dclp, Chroma) through the objective and fluorescence was observed through a 605 nm band-pass filter (D605/55, Chroma). Supported lipid bilayers and GUVs stained with DiD were illuminated through a 620 nm (ET620/60, Chroma) and via a dichroic mirror (660dclp, Chroma), and observed through a 665 nm band-pass filter (HQ665/60, Chroma).

Supplementary Material

Refer to Web version on PubMed Central for supplementary material.

Acknowledgments

This work was supported by NIH grant R01 AI30577 (LKT) and R21 AI103601 (JMW). We thank Elizabeth Nelson for technical help with the production of pseudoviruses.

References

1. Singer SJ, Nicolson GL. The fluid mosaic model of the structure of cell membranes. Science. 1972; 175:720–731. [PubMed: 4333397]
2. Engelman DM. Membranes are more mosaic than fluid. Nature. 2005; 438:578–580. [PubMed: 16319876]
3. Kiessling V, Wan C, Tamm LK. Domain coupling in asymmetric lipid bilayers. Biochim Biophys Acta. 2009; 1788:64–71. [PubMed: 18848518]
4. Simons K, Ikonen E. Functional rafts in cell membranes. Nature. 1997; 387:569–572. [PubMed: 9177342]
5. Brown DA, London E. Functions of lipid rafts in biological membranes. Annu Rev Cell Dev Biol. 1998; 14:111–136. [PubMed: 9891780]

6. Pike LJ. The challenge of lipid rafts. J Lipid Res. 2009; 50(Suppl):S323–S328. [PubMed: 18955730]
7. Jacobson K, Mouritsen OG, Anderson RGW. Lipid rafts: at a crossroad between cell biology and physics. Nat Cell Biol. 2007; 9:7–14. [PubMed: 17199125]
8. Baumgart T, Hess ST, Webb WW. Imaging coexisting fluid domains in biomembrane models coupling curvature and line tension. Nature. 2003; 425:821–824. [PubMed: 14574408]
9. Campbell SM, Crowe SM, Mak J. Lipid rafts and HIV-1: from viral entry to assembly of progeny virions. J Clin Virol. 2001; 22:217–227. [PubMed: 11564586]
10. Liao Z, Cimakasky LM, Hampton R, Nguyen DH, Hildreth JE. Lipid rafts and HIV pathogenesis: host membrane cholesterol is required for infection by HIV type 1. AIDS Res Hum Retroviruses. 2001; 17:1009–1019. [PubMed: 11485618]
11. White JM, Delos SE, Brecher M, Schornberg K. Structures and mechanisms of viral membrane fusion proteins: multiple variations on a common theme. Crit Rev Biochem Mol Biol. 2008; 43:189–219. [PubMed: 18568847]
12. Wilen CB, Tilton JC, Doms RW. Molecular mechanisms of HIV entry. Adv Exp Med Biol. 2012; 726:223–242. [PubMed: 22297516]
13. Melikyan GB. HIV entry: a game of hide-and-fuse? Curr Opin Virol. 2014; 4:1–7. [PubMed: 24525288]
14. Chernomordik LV, Kozlov MM. Mechanics of membrane fusion. Nat Struct Mol Biol. 2008; 15:675–683. [PubMed: 18596814]
15. Harrison SC. Viral membrane fusion. Nat Struct Mol Biol. 2008; 15:690–698. [PubMed: 18596815]
16. Bartesaghi A, Merk A, Borgnia MJ, Milne JL, Subramaniam S. Prefusion structure of trimeric HIV-1 envelope glycoprotein determined by cryo-electron microscopy. Nat Struct Mol Biol. 2013; 20:1352–1357. [PubMed: 24154805]
17. Julien JP, et al. Crystal structure of a soluble cleaved HIV-1 envelope trimer. Science. 2013; 342:1477–1483. [PubMed: 24179159]
18. Tamm LK, Lee J, Liang B. Capturing glimpses of an elusive HIV gp41 prehairpin fusion intermediate. Structure. 2014; 22:1225–1226. [PubMed: 25185826]
19. Doms RW, Moore JP. HIV-1 membrane fusion: targets of opportunity. J Cell Biol. 2000; 151:F9–F14. [PubMed: 11038194]
20. Waheed AA, Freed EO. Lipids and membrane microdomains in HIV-1 replication. Virus Res. 2009; 143:162–176. [PubMed: 19383519]
21. Graham DR, Chertova E, Hilburn JM, Arthur LO, Hildreth JE. Cholesterol depletion of human immunodeficiency virus type 1 and simian immunodeficiency virus with beta-cyclodextrin inactivates and permeabilizes the virions: evidence for virion-associated lipid rafts. J Virol. 2003; 77:8237–8248. [PubMed: 12857892]
22. Dietrich C, et al. Lipid rafts reconstituted in model membranes. Biophys J. 2001; 80:1417–1428. [PubMed: 11222302]
23. Crane JM, Tamm LK. Role of cholesterol in the formation and nature of lipid rafts in planar and spherical model membranes. Biophys J. 2004; 86:2965–2979. [PubMed: 15111412]
24. Han X, Tamm LK. A host-guest system to study structure-function relationships of membrane fusion peptides. Proc Natl Acad Sci U S A. 2000; 97:13097–13102. [PubMed: 11069282]
25. Tamm LK, Han X. Viral fusion peptides: a tool set to disrupt and connect biological membranes. Biosci Rep. 2000; 20:501–518. [PubMed: 11426691]
26. Brugger B, et al. The HIV lipidome: a raft with an unusual composition. Proc Natl Acad Sci U S A. 2006; 103:2641–2646. [PubMed: 16481622]
27. Tamm, LK. Cell entry of influenza virus by membrane fusion. In: Schmidt, MFG., editor. Influenza Viruses – Facts and Perspectives. Berlin: Grosse Verlag; 2007. p. 48-55.
28. Feigenson GW. Phase behavior of lipid mixtures. Nat Chem Biol. 2006; 2:560–563. [PubMed: 17051225]

29. Domanska MK, Kiessling V, Stein A, Fasshauer D, Tamm LK. Single vesicle millisecond fusion kinetics reveals number of SNARE complexes optimal for fast SNARE-mediated membrane fusion. J Biol Chem. 2009; 284:32158–32166. [PubMed: 19759010]
30. Kiessling V, et al. Rapid fusion of synaptic vesicles with reconstituted target SNARE membranes. Biophys J. 2013; 104:1950–1958. [PubMed: 23663838]
31. Kilby JM, et al. Potent suppression of HIV-1 replication in humans by T-20, a peptide inhibitor of gp41-mediated virus entry. Nat Med. 1998; 4:1302–1307. [PubMed: 9809555]
32. Eggeling C, et al. Direct observation of the nanoscale dynamics of membrane lipids in a living cell. Nature. 2009; 457:1159–1162. [PubMed: 19098897]
33. de Almeida RF, Fedorov A, Prieto M. Sphingomyelin/phosphatidylcholine/cholesterol phase diagram: boundaries and composition of lipid rafts. Biophys J. 2003; 85:2406–2416. [PubMed: 14507704]
34. Honerkamp-Smith AR, et al. Line tensions, correlation lengths, and critical exponents in lipid membranes near critical points. Biophys J. 2008; 95:236–246. [PubMed: 18424504]
35. Veatch SL, et al. Critical fluctuations in plasma membrane vesicles. ACS Chem Biol. 2008; 3:287–293. [PubMed: 18484709]
36. Zhao J, Wu J, Veatch SL. Adhesion stabilizes robust lipid heterogeneity in supercritical membranes at physiological temperature. Biophys J. 2013; 104:825–834. [PubMed: 23442961]
37. Machta BB, Papanikolaou S, Sethna JP, Veatch SL. Minimal model of plasma membrane heterogeneity requires coupling cortical actin to criticality. Biophys J. 2011; 100:1668–1677. [PubMed: 21463580]
38. Edidin M. The state of lipid rafts: from model membranes to cells. Annu Rev Biophys Biomol Struct. 2003; 32:257–283. [PubMed: 12543707]
39. Lai AL, Moorthy AE, Li Y, Tamm LK. Fusion activity of HIV gp41 fusion domain is related to its secondary structure and depth of membrane insertion in a cholesterol-dependent fashion. J Mol Biol. 2012; 418:3–15. [PubMed: 22343048]
40. Qiang W, Weliky DP. HIV fusion peptide and its cross-linked oligomers: efficient syntheses, significance of the trimer in fusion activity, correlation of beta strand conformation with membrane cholesterol, and proximity to lipid headgroups. Biochemistry. 2009; 48:289–301. [PubMed: 19093835]
41. Lipowsky R. Domain-induced budding of fluid membranes. Biophys J. 1993; 64:1133–1138. [PubMed: 19431884]
42. Garcia-Saez AJ, Chiantia S, Schwille P. Effect of line tension on the lateral organization of lipid membranes. J Biol Chem. 2007; 282:33537–33544. [PubMed: 17848582]
43. Jensen MH, Morris EJ, Simonsen AC. Domain shapes, coarsening, and random patterns in ternary membranes. Langmuir. 2007; 23:8135–8141. [PubMed: 17590026]
44. Tayebi L, et al. Long-range interlayer alignment of intralayer domains in stacked lipid bilayers. Nat Mater. 2012; 11:1074–1080. [PubMed: 23085566]
45. Moissoglu K, et al. Regulation of Rac1 translocation and activation by membrane domains and their boundaries. J Cell Sci. 2014; 127:2565–2576. [PubMed: 24695858]
46. Chamberlain LH, Burgoyne RD, Gould GW. SNARE proteins are highly enriched in lipid rafts in PC12 cells: implications for the spatial control of exocytosis. Proc Natl Acad Sci U S A. 2001; 98:5619–5624. [PubMed: 11331757]
47. Murray DH, Tamm LK. Clustering of syntaxin-1A in model membranes is modulated by phosphatidylinositol 4,5-bisphosphate and cholesterol. Biochemistry-Us. 2009; 48:4617–4625.
48. Mukai A, et al. Dynamic clustering and dispersion of lipid rafts contribute to fusion competence of myogenic cells. Exp Cell Res. 2009; 315:3052–3063. [PubMed: 19615358]
49. Ishii M, et al. RANKL-induced expression of tetraspanin CD9 in lipid raft membrane microdomain is essential for cell fusion during osteoclastogenesis. J Bone Miner Res. 2006; 21:965–976. [PubMed: 16753027]
50. Sleight SB, et al. Isolation and proteomic analysis of mouse sperm detergent-resistant membrane fractions: evidence for dissociation of lipid rafts during capacitation. Biol Reprod. 2005; 73:721–729. [PubMed: 15917346]

51. Angelova MI, Dimitrov DS. Liposome electroformation. Faraday Discuss Chem SOC. 1986; 81:303–311.

52. Wagner ML, Tamm LK. Tethered polymer-supported planar lipid bilayers for reconstitution of integral membrane proteins: silane-polyethyleneglycol-lipid as a cushion and covalent linker. Biophys J. 2000; 79:1400–1414. [PubMed: 10969002]

53. Struck DK, Hoekstra D, Pagano RE. Use of resonance energy transfer to monitor membrane fusion. Biochemistry. 1981; 20:4093–4099. [PubMed: 7284312]

54. Kiessling V, Crane JM, Tamm LK. Transbilayer effects of raft-like lipid domains in asymmetric planar bilayers measured by single molecule tracking. Biophys J. 2006; 91:3313–3326. [PubMed: 16905614]

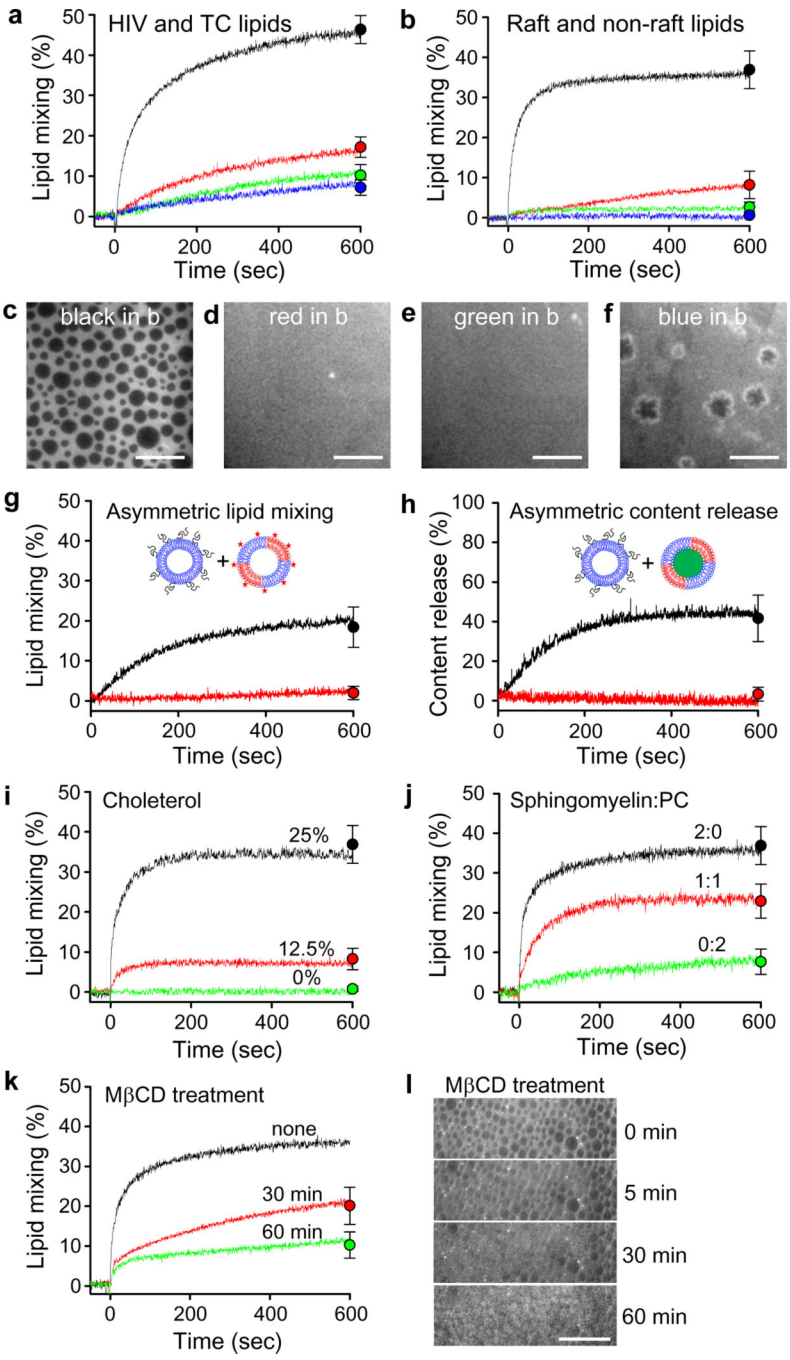

Figure 1.

Phase-separated domains and cholesterol are required for HIV-FP to fuse HIV envelope (HIV) and T-cell (TC) membrane-mimicking lipid mixtures. **(a)** HIV-FP-mediated lipid mixing of a 1:9 mixture of 1% NBD-PE/Rh-PE labeled HIV and unlabeled TC liposomes (black). In the absence of cholesterol in HIV (red) or TC (green) or both (blue) liposomes fusion was greatly reduced. **(b)** HIV-FP-mediated fusion of liposomes composed of bSM/bPS/Ch (2:1:1) (black), bPC/bPS/Ch (2:1:1) (red), bPC/bPS (3:1) (green), and bSM/bPS (3:1) (blue). **(c–f)** Fluorescence micrographs of 0.1 mol% Rh-PE stained

supported bilayers composed of bSM/bPS/Ch (2:1:1) (**c**), bPC/bPS/Ch (**d**), bPC/bPS (3:1) (**e**), and bSM/bPS (3:1) (**f**). Scale bars are 20 m. **(g)** 45 μM unlabeled bPC/bPS (3:1) were preincubated with HIV-FP and then added to 5 μM NBD-PE/Rh-PE-labeled liposomes composed of bSM/bPS/Ch (2:1:1) (black) or bPC/bPS (3:1) (red). **(h)** Same as (**g**) but with ANTS/DPX-labeled liposomes. **(i)** HIV-FP-mediated fusion of bSM/bPS (2:1) HIV-FP pre-incubated liposomes with 0% (green), 12.5% (red), and 25% (black) cholesterol. **(j)** HIV-FP-mediated fusion of liposomes composed of bSM/bPC/bPS/Ch in molar ratios of 0:2:1:1 (green), 1:1:1:1 (red), and 2:0:1:1 (black). **(k)** HIV-FP-mediated fusion of bSM/bPS/Ch (2:1:1) liposomes before (black) and after 30 (red) or 60 (green) min treatment with 5 mM MβCD. **(l)** Fluorescence micrographs of same area of a supported bSM/bPS/Ch (2:1:1) bilayer at indicated times after addition of 5 mM MβCD. Scale bar is 10 m. Total liposome concentrations were 50 μM in all experiments and FP concentrations were 2 μM, except in (**a**) where it was 1 μM.

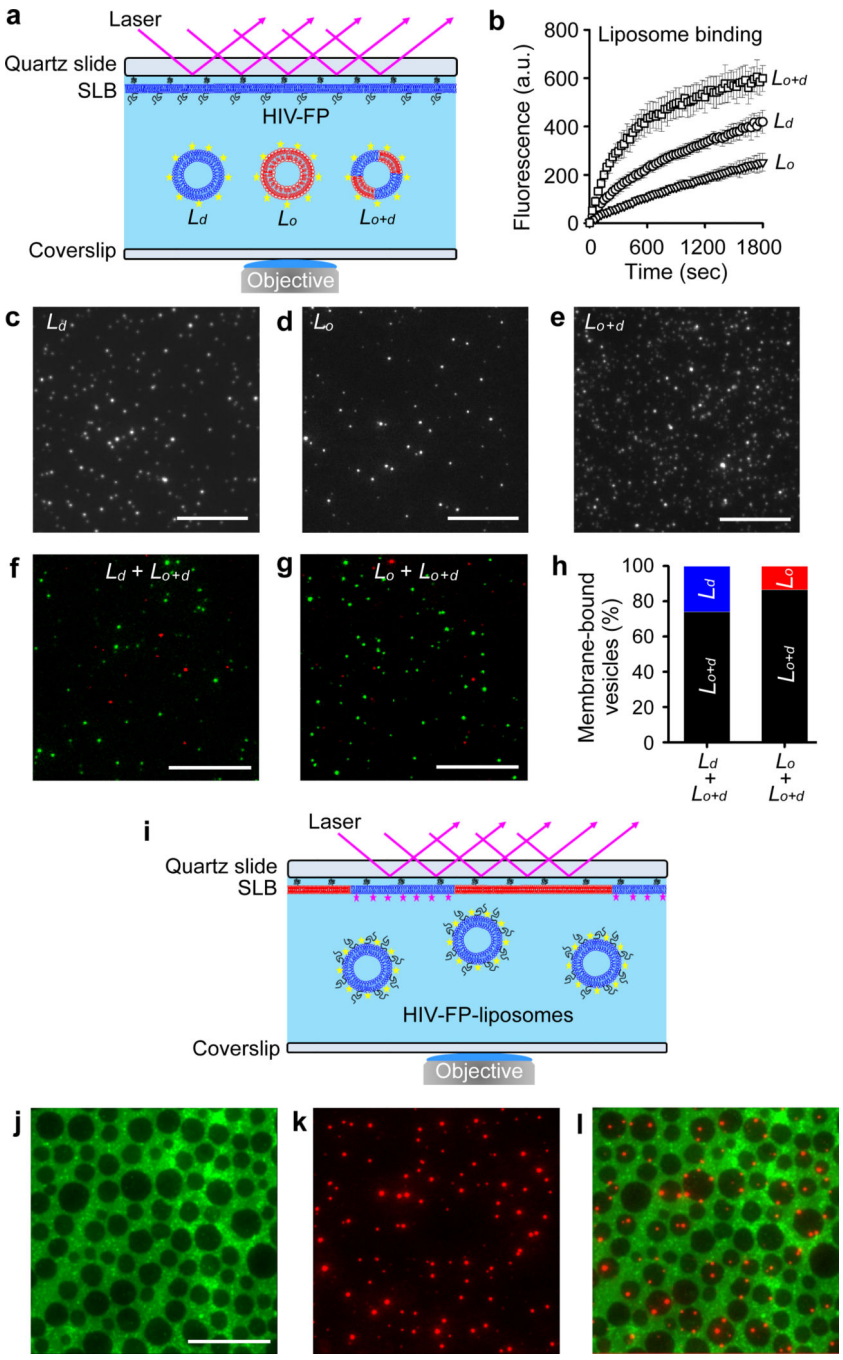

Figure 2.

Membrane-bound HIV-FP preferentially binds phase-separated L_{o+d} liposomes and targets L_o/L_d phase boundaries in phase-separated membranes. **(a)** Schematic of TIRF microscopy to measure the binding of liposomes to supported membranes preincubated with HIV-FP. **(b)** Time course of mean fluorescence intensity recorded by TIRF microscopy measuring the binding of bPC/bPS (3:1, L_d), bSM/DPPS/Ch (2:1:1, L_o), and bSM/DOPS/Ch (2:1:1, L_{o+d}) liposomes to HIV-FP-doped supported bilayers. TIRF micrographs of bound L_d (**c**), L_o (**d**), or L_{o+d} (**e**) liposomes captured 10 min after liposome addition. **(f–h)** Competitive binding of

two types of liposomes to HIV-FP-doped supported bilayers. 0.2 M L_d (**f**) or L_o (**g**) liposomes were added simultaneously with equal amounts of L_{o+d} liposomes to the supported membranes. Green spots indicate L_{o+d} liposomes labeled with 0.1 mol% Rh-PE and red spots indicate L_d or L_o liposomes labeled with 0.5 mol% DiD. **(h)** Quantitative analysis of bound fractions of each type of liposome in **f** and **g**. **(i)** Schematic of TIRF microscopy to determine the locations HIV-FP-targeted liposomes to different regions of supported two-phase bilayers composed of bSM/bPS/Ch (2:1:1). Liposomes composed of bPC/bPS (3:1) were pre-incubated with HIV-FP and then allowed to bind to the supported membrane. (**j**) Epifluorescence micrograph of supported membrane stained with 0.1 mol% Rh-PE. (**k**) TIRF micrograph of bound 0.5 mol% DiD labeled liposomes as mediated by HIV-FP. The overlay image (**l**) shows that most liposomes favor the boundaries between L_d and L_o phases (see also Supplementary Fig. 4). All scale bars are 20 m.

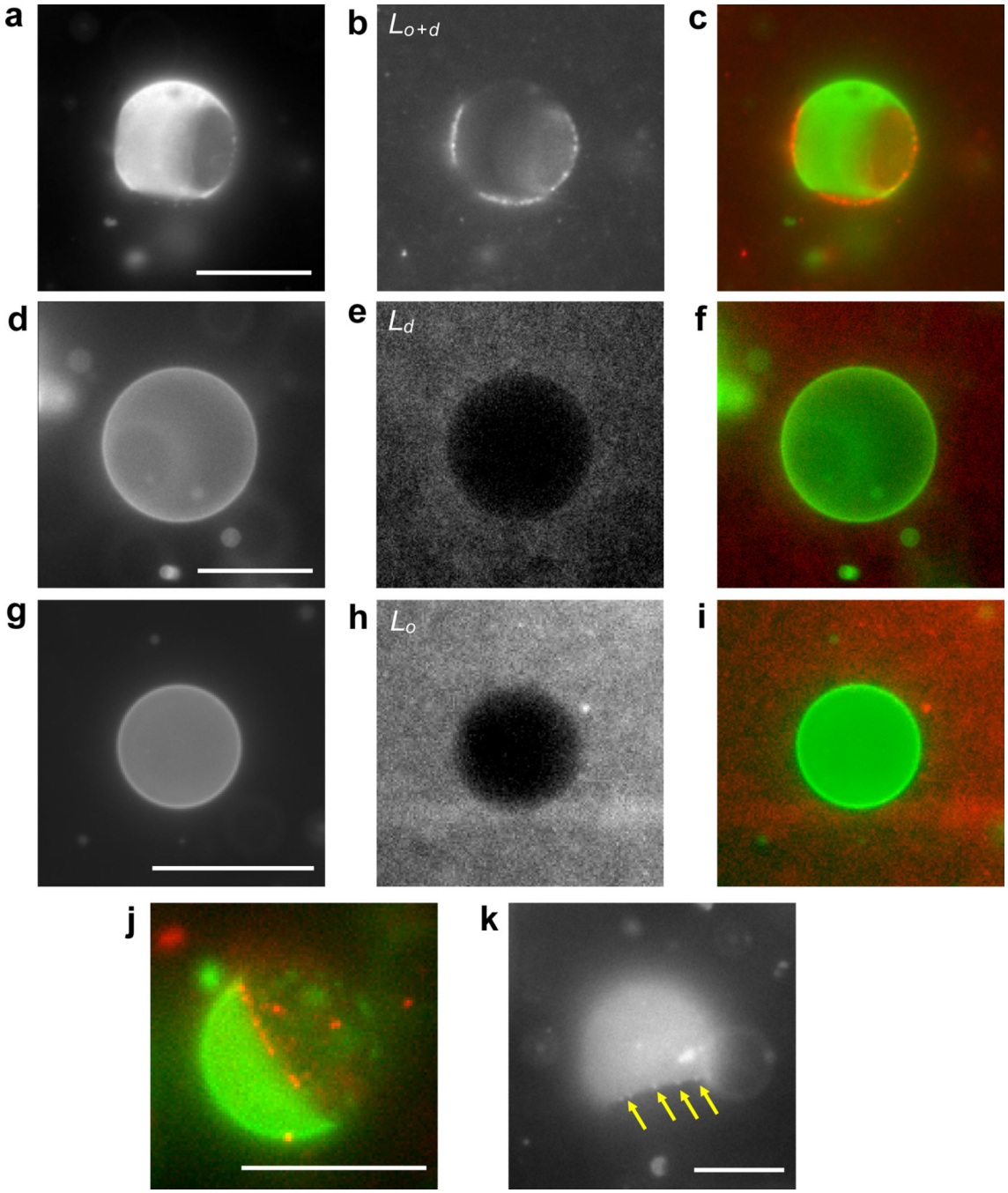

Figure 3.

HIV-FP-liposomes are targeted to L_o/L_d phase boundary regions in GUVs. Fluorescence micrographs of GUVs labeled with 0.1 mol% Rh-PE (**a,d,g**) and LUV liposomes labeled with 0.5 mol% DiD (**b,e,h**). GUVs were composed of bSM/DOPC/Ch (2:2:1) for L_{o+d} **(a–c)**, bPC for L_d **(d–f)**, or bSM/Ch (2:1) for L_o **(g–i)** phase bilayers. LUVs were composed of bPC/bPS (3:1) and pre-incubated for 10 min with HIV-FP before they were added to the GUVs. Images were taken after 30 min of incubation at room temperature. (**c,f,i**) are two-color overlays of the other panels in the same row. (**j**) Fluorescence micrograph showing

HIV-FP-mediated binding of LUVs to the phase boundary region of a L_{o+d} phase-separated GUV membrane. The overlays show GUV phase behavior in green and the bound LUVs in red. (**k**) Fluorescence micrograph of HIV-FP-LUVs bound to the phase boundary region of a phase-separated L_{o+d} GUV membrane. In this experiment, LUVs and GUVs were labeled with Rh-PE for simultaneous observation. Several bright spots representing LUVs indicated by yellow arrows are observed concentrated at a domain boundary. Scale bars are 20 m.

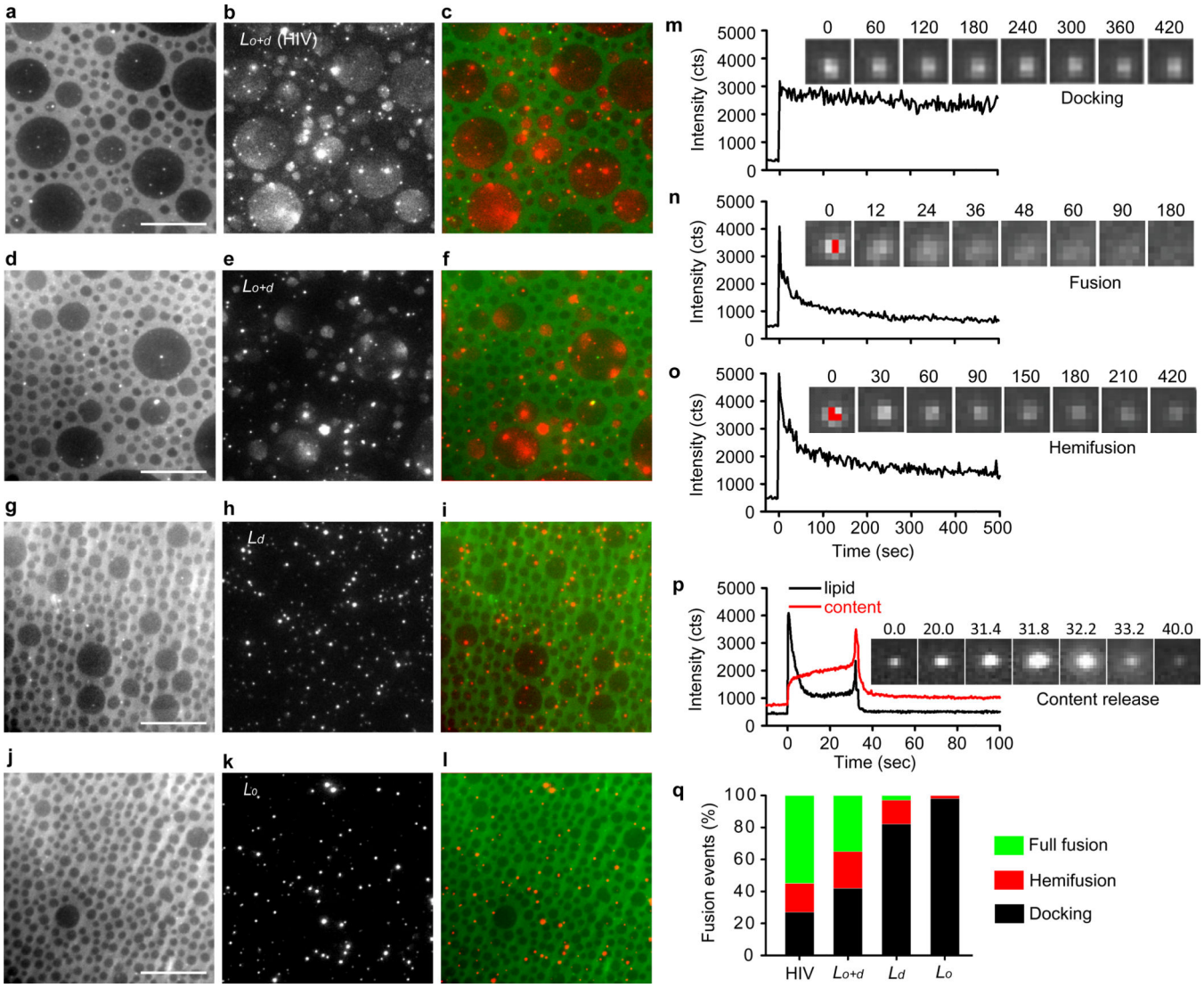

Figure 4.

HIV-FP-liposomes fuse at L_o/L_d phase boundaries in supported membranes. Rh-PE-labeled supported bilayers composed of bSM/bPC/Ch (2:2:1) (**a,d,g,j**) were incubated with 5 M HIV-FP for 10 min. DiD-labeled liposomes composed of HIV lipids (**b**), bSM/DOPS/Ch (2:1:1) **(e)** both for L_{o+d}, bPC/bPS (3:1) (**h**) for L_d, or bSM/DPPS/Ch (2:1:1) **(k)** for L_o phase bilayers were added and observed by TIRF microscopy. The overlayed images show that L_{o+d} liposomes (red) (**c,f**), but not L_d or L_o liposomes (**i,l**) fused with supported bilayers (green). Scale bars are 20 m. **(m,n,o)** different typical fluorescence behaviors of single bound liposomes: **(m)** constant fluorescence corresponding to binding without fusion (docking), **(n)** complete fluorescence decay corresponding to full fusion, and **(o)** fluorescence decay to ~50% of original corresponding to hemifusion. Time zero was defined as the first frame with a visible liposome. TIRF images of single liposomes at representative times (sec) are shown in 2.5 × 2.5 μm^2 insets. (**p**) Fluorescence time course of a single DiD- and sulforhodamine B-labeled liposome. Binding and lipid spread (black), and content release (red) were recorded simultaneously in respective channels. Content release was

tracked by integrating the fluorescence intensity from the vesicle area. The 5 × 5 μm^2 insets show TIRF images of content release from the single liposome at representative times (sec). (**q**) Relative frequencies of different events: binding without fusion/docking (black), hemifusion (red), and full fusion (green).

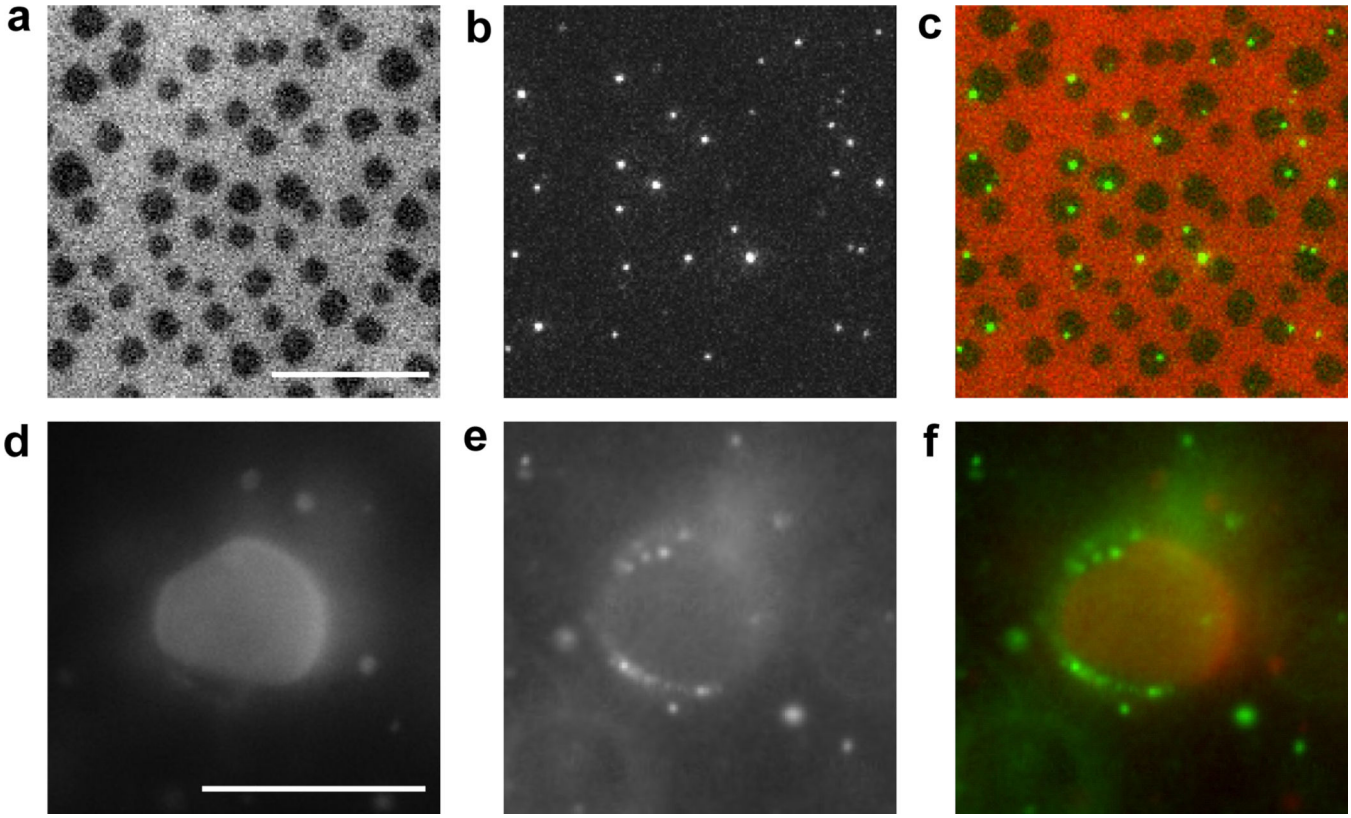

Figure 5.

HIV-1 pseudoviruses bind preferentially to L_o/L_d phase boundaries in supported lipid bilayers or GUVs composed of bSM/DOPC/Ch (2:2:1). Fluorescence micrographs of a supported bilayer (**a–c**) and a GUV (**d–f**) labeled with 0.1 mol% DiD (**a,d**) and HIV pseudoviruses labeled with gag-mKO (**b,e**), and two-color overlays (**c,f**). HIV pseudoviruses were preincubated with enfuvirtide at 55 C for 30 min and then added to both lipid bilayers. Images of membrane-bound HIV pseudoviruses were taken after 30 min incubation at room temperature. The overlays show the preferential binding of the HIV particles to the L_o/L_d boundary regions of the phase-separated membranes. Scale bars are 20 m.

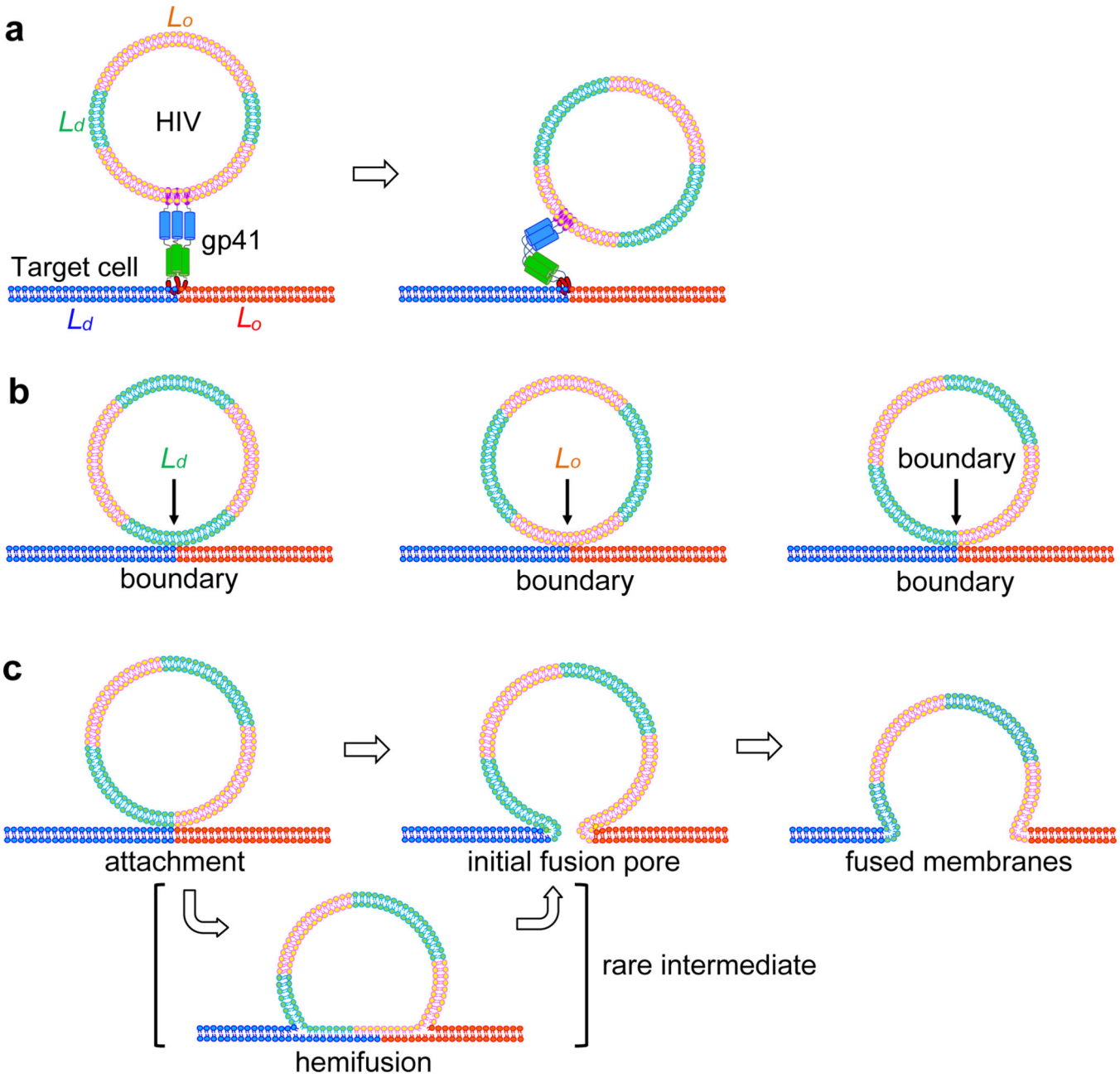

Figure 6.

Lipid domain boundaries in viral and cellular target membranes promote HIV gp41-mediated membrane fusion. (**a**) Targeting of HIV particles to domain boundaries of two-phase lipid bilayers. The exposed fusion peptides of gp41 in the triggered pre-hairpin intermediate interact with the domain boundaries of the target cell membrane. (**b**) Three possible configurations of L_o/L_d phase lipid bilayer attachments: L_d-boundary (left), L_o-boundary (center), and boundary-boundary (right). Membrane fusion is most efficient in the boundary-boundary attachment configuration. (**c**) Proposed mechanism of membrane fusion at L_o/L_d lipid domain boundaries: The boundary-boundary attachment configuration lowers the energy required to open the initial fusion pore, which later expands to a fully fused

membrane. Hemifusion intermediates are sometimes seen in this configuration. They may be caused by lipid asymmetry of the host and viral membrane-derived hemifusion diaphragm. In this model, the hemifusion state is resolved by shifting phase-mismatched leaflets back into register and thereby opening the initial fusion pore.